Available online at www.sciencedirect.com
SCIENCE DIRECT®
Bioorganic & Medicinal Chemistry 13 (2005) 5581–5591
Bioorganic & Medicinal Chemistry

Binding studies and GRIND/ALMOND-based 3D QSAR analysis of benzothiazine type K_{ATP}-channel openers

Emanuele Carosati,[a] Horst Lemoine,[b] Roberto Spogli,[c] Dagmar Grittner,[b] Raimund Mannhold,[b] Oriana Tabarrini,[c] Stefano Sabatini[c] and Violetta Cecchetti[c,*]

[a]*Laboratorio di Chemiometria e Chemioinformatica, Dipartimento di Chimica, Università di Perugia, Via Elce di Sotto 10, I-06123 Perugia, Italy*
[b]*Department of Laser Medicine, Molecular Drug Research Group, Heinrich-Heine-Universität, Universitätsstr.1, D-40 225 Düsseldorf, Germany*
[c]*Dipartimento di Chimica e Tecnologia del Farmaco, Università di Perugia, Via del Liceo 1, I-06123 Perugia, Italy*

Received 14 March 2005; revised 27 May 2005; accepted 3 June 2005
Available online 5 July 2005

Abstract—For seventeen 1,4-benzothiazine potassium channel openers, we performed binding studies in rat aortic smooth muscle cells and cardiomyocytes, compared their binding affinities with published relaxation data, and derived 3D-QSAR models using GRIND/ALMOND descriptors. Binding affinities in smooth muscle cells range from a pK_D of 4.76 for compound **3e** to 9.10 for compound **4c**. Comparison of data for smooth muscle relaxation and binding shows preferentially higher pEC_{50}s for the former. In cardiomyocytes, pK_D values range from 4.21 for **3e** to 8.16 for **4c**. 3D-QSAR analysis resulted in PLS models of two latent variables for all three activities with determination coefficients of 0.97 (smooth muscle relaxation) and 0.94 (smooth muscle cells- and cardiomyocytes-binding). Internal validation yielded q^2 values of 0.69, 0.66, and 0.64. The carbonyl on the N-4 substituent, the hydrogen bond acceptor at C-6, the five-membered ring at N-4, and the *gem*-dimethyls mainly guide strong binding and strong smooth muscle relaxation.

1. Introduction

ATP-sensitive potassium channels (K_{ATP}-channels) are members of the subfamily of inward rectifiers Kir,[1] which exhibit a stronger inward than outward conductance at a given membrane potential. K_{ATP}-channels differ from other inward rectifiers by including a regulatory β-subunit, the sulfonylurea receptor protein SUR[2] in addition to the channel forming α-subunit Kir. K_{ATP}-channels are widely distributed in various organs and exhibit many physiological functions, such as reduction of action potential duration[3] in cardiomyocytes,[4] regulation of insulin secretion[5] in β-cells of the pancreas,[6] and control of vessel tone[7] in smooth muscle cells[8] and transmitter release[9] in neurons.[10] Given their many physiological functions, K_{ATP}-channels represent promising drug targets. Both antagonists, such as the antidiabetic sulfonylureas as well as activators or openers of K_{ATP}-channels (KCOs), have been described.[11] Interest in the KCOs arose in the 1980s when cromakalim,[12] pinacidil,[13] and nicorandil[14] were shown to relax smooth vascular muscle via K_{ATP}-channel opening. Thus, these agents were first indicated for the treatment of hypertension and angina pectoris; this was later extended to include other diseases such as asthma,[15] urinary incontinence,[16] and baldness.[17] KCOs were also shown to protect cells against cardiac ischemia,[18] and to influence lipid metabolism.[19] The therapeutic usefulness of KCOs depends on their tissue selectivity. The existence and organ-specific distribution of isoforms of the K_{ATP}-channel forming subunits Kir (Kir 6.1[20] and Kir 6.2[21]) and SUR (SUR1,[22] SUR2A,[23] and SUR2B[24]) might represent a rational basis for detecting tissue-selective KCOs. The identification of the KCO-binding site on sulfonylurea receptors represents a further step in this direction.[25]

Potassium channel openers are very heterogeneous in chemical structure.[26] First generation KCOs include

Keywords: K_{ATP}-channel openers; Binding studies; Smooth muscle relaxation; GRIND/ALMOND analysis.
* Corresponding author. Tel.: +39 075 585 5153; fax: +39 075 585 5115; e-mail: viola@unipg.it

0968-0896/$ - see front matter © 2005 Elsevier Ltd. All rights reserved.
doi:10.1016/j.bmc.2005.06.010

benzopyrans, thioformamides, and cyanoguanidines.[27] Second generation KCOs include, for example, tertiary carbinols and dihydropyridine related structures.[27] Benzopyrans represent the most intensively investigated subgroup. In many structure–activity studies the different positions of the benzopyran ring have been variously substituted resulting in an optimized bioactivity.[28] The benzopyran nucleus itself has also been modified in both the aromatic ring and in the pyran moiety. In a search for new KCO chemotypes, Cecchetti et al.[29] examined the effect of replacing the benzopyran with a 1,4-benzothiazine nucleus and detected compounds with very high smooth muscle relaxing potency.

In this study, we performed binding studies with the above-mentioned 1,4-benzothiazine KCOs in aortic smooth muscle cells and cardiac membranes of rat, compared their binding affinities with formerly measured smooth muscle relaxation data, and derived QSAR models applying GRIND descriptors.[30]

2. Dataset and methodology

2.1. Dataset

The dataset comprises seventeen 1,4-benzothiazines with main variations in 4- and 6-positions. 4-Substitution includes cyclic moieties such as pyrrolidinone, piperidinone, and cyclopentenone, as well as non-cyclic ketones and amides. Small, electron-withdrawing substituents such as Br, CN, NO_2, and CF_3 are used in 6-position. As a reference compound, levcromakalim is included in the dataset.

2.2. Biological methods

2.2.1. Tissue preparation. Male Wistar rats (body weight 200–300 g) were anesthetized with ether; after opening the chest, heart and aorta were removed and perfused with modified Krebs solution containing (mmol/l) 89.0 NaCl, 29.0 $NaHCO_3$, 5.0 KCl, 1.0 Na_2HPO_4, 0.5 $MgSO_4$, 0.04 EDTA, and 2.25 $CaCl_2$ equilibrated with carbogen (95% O_2/5% CO_2). The water was deionized and double-distilled in glass. After the removal of connective tissue, fat, and endothelium under sterile conditions, the aortas were cut into rings of 1 mm width and transferred into tissue culture dishes. Hearts were mounted on a Langendorff apparatus for the retrograde perfusion of coronary arteries.

2.2.2. Cell culture of aortic myocytes. Aortic rings were explanted in 6-well cell culture dishes (Corning, NY, USA) covered with a thin layer of medium according to Ross,[31] and put into an incubator gassed with 93% O_2 and 7% CO_2. The medium (Dulbecco's modified Eagle's medium (DMEM), Gibco, Inchinnan Scotland) was supplemented with 10% fetal calf serum (FCS), 2 mmol/l glutamate, 10 mmol/l HEPES, 100 U/ml penicillin, and 100 μg/ml streptomycin. After 3–4 h, the rings stuck to the bottom of the 6-well dishes and were covered with medium. After ~10–14 days, when the cells had grown out of the aortic rings, the rings were removed and the cells were passaged (i.e., passage 1) into 75 cm^2 cell culture flasks (Nunc, Roskilde, Denmark) using 0.05% trypsin and 0.02% EDTA. After having reached confluency after 5–7 days, the cells were passaged (i.e., passage 2) into 24-well dishes (Corning, NY, USA) to perform radioligand binding experiments with [^{3}H]P1075.

2.2.3. Isolation of cardiomyocytes. Isolated myocytes were prepared according to Buxton and Brunton[32] with some modifications. After cannulation of the aorta, hearts were mounted on a perfusion apparatus. Warm (37 °C) Ca^{2+}-free salt solution containing (mmol/l) 35.0 NaCl, 25.0 $NaHCO_3$, 4.7 KCl, 1.2 KH_2PO_4, 20.0 Na_2HPO_4, 10.0 HEPES, 133.2 sucrose, and 10.0 glucose, continually gassed with carbogen (95% O_2/5% CO_2), was perfused through the heart for 5 min. Thus, the hearts were washed free of all blood cells and ceased beating. Thereafter, the perfusate was supplemented with 0.5 mg/ml collagenase and 1.5 mg/ml hyaluronidase. Twenty to thirty minutes after the start of enzyme perfusion, the flaccid ventricles were gently dissected and teased into small pieces, placed in a petri dish with fresh enzyme solution, and incubated again at 37 °C in a shaking water bath for 5–10 min. After complete disaggregation of ventricles, the cell suspension was decanted through a sieve and centrifuged at 100*g* for 2 min. The resulting pellet was resuspended in a buffer containing (mmol/l) 130.0 NaCl, 4.7 KCl, 1.2 KH_2PO_4, 20.0 Na_2HPO_4, 25.0 HEPES, and 10.0 glucose complemented with 2% albumin (fraction V). Further purification of the cells was achieved by sedimentation of the cells, for 10 min, in 13 ml polycarbonated tube and by discarding the supernatant. Loose pellets were purified for the second time by sedimentation and then resuspended in MEMS (Minimum Essential Medium Eagle) with a cell concentration of 0.1 mio/ml. From one heart, 5–7 million cells were isolated, with a yield of more than 70% rod-shaped cells able to exclude trypan blue. Incubations for radioligand binding were done in siliconized flat-bottomed glass tubes at 37 °C for 60 min.

2.2.4. Radioligand binding. Rat aortic smooth muscle cells (RASMC) cultured in 24-well cell culture dishes were incubated in a total volume of 200 μl Hanks' balanced salt solution (HBSS) containing (mmol/l) 137.0 NaCl, 5.4 KCl, 1.2 $MgSO_4$, 0.34 Na_2HPO_4, 4.2 $NaHCO_3$, 0.44 KH_2PO_4, 20.0 HEPES, 5.5 glucose, 1.3 $CaCl_2$. Enzymatically disaggregated cardiomyocytes were incubated in a physiological salt solution containing (mmol/l) 130.0 NaCl, 4.75 KCl 5.0 $MgCl_2$, 1.19 KH_2PO_4, 20.0 HEPES, 5.0 glucose, and 0.2 % BSA (fraction V) in a total volume of 200 μl containing 50,000 myocytes. K_{ATP}-channels were radiolabeled with [^{3}H]P1075 *N*-cyano-*N*′-[1,1-dimethyl-[2,2,3,3-^{3}H]propyl]-*N*″-(3-pyridinyl)guanidine,[33,34] with a specific activity of 108 Ci/mmol. The reaction was initiated by addition of the radioligand; binding observed in the presence of 1 μmol/l P 1075 was regarded as non-specific. In RASMC, binding was stopped by suction of the incubation medium followed by five successive washings with cold HBSS-solution. The cell-bound ligand was transferred to scintillation vials after incubation of the

cell monolayers with 1 mol/l NaOH for 30 min at 60 °C. In cardiomyocytes, bound radioligand was separated from free radioligand by rapid vacuum filtration through Whatman GF/A glass fiber filters. The filters were rapidly washed eight times with 2 ml ice-cold buffer (10 mmol/l Tris, 5 mmol/l $MgCl_2$, pH 8.0) and transferred to scintillation vials. After addition of 3 ml scintillation fluid (Ultima Gold, Packard, USA) the vials were vigorously shaken for 1 h and counted in a scintillation counter (Packard 1500) with 50% efficiency. Competition binding experiments were performed in the presence of 1 nmol/l [^{3}H]P1075 ([L*]) and increasing concentrations of competing ligands [L]. Displacement curves were analyzed by non-linear regression as reported[35,36] according to the following equation:

$$B_s([L]) = B_0 - B_0[L]/\{[L] + K_D(1 + [L^*]/K_L^*)\} \quad (1)$$

where B_0 and B_s([L]) represent the specific binding of L* to K_{ATP}-channels in the absence and presence of L, K_L^* denotes the dissociation constant of the radioligand L*, and K_D is the equilibrium dissociation constant of the test compound L. Experimental data were analyzed after transformation of data to obtain homoscedasticity which resulted in reliable estimates of parameters (B_0, B_{ns}, and pK_D) and asymptotic standard deviations (ASD). Data were fitted to the hyperbola defined by Eq. 1 by non-linear regression using the SAS software package STAT. Data points in the figures are means ± SEM.

2.2.5. Drugs and materials. [^{3}H]P1075 (108 Ci/mmol = 4.00 TBq/mmol) was purchased from the Radiochemical Center, Amersham, UK. P 1075 and bimakalim were generous gifts from Leo (Ballerup, Denmark) and E. Merck (Darmstadt, D). Stock solutions of KCOs were dissolved in DMSO. DMSO-concentration did not exceed 0.3% (v/v) in radioligand binding. Other chemicals were obtained from local commercial sources.

2.3. Molecular modeling methods

2.3.1. Geometry optimization. The geometry of the dataset compounds was optimized via ab initio Molecular Orbital (MO) calculations using GAUSSIAN98 software.[37] Geometry optimization was performed with the B3LYP density functional method,[38] using the 6-31 G basis set. All the MO calculations were run on a linux machine equipped with a Pentium 4 processor and a 2 GB memory.

2.3.2. Chemical descriptors. GRid-INdependent Descriptors (GRIND)[30] were generated, analyzed, and interpreted using the version 3.3 of the program ALMOND.[39] GRIND have been designed mainly to represent pharmacodynamic properties; they start from molecular interaction fields (MIF) computed on the basis of the GRID force field.[40] When MIF are computed for a dataset molecule, the nodes showing favorable energies of probe–molecule interaction represent positions where groups of a receptor, mimed by the probe, would interact favorably with the molecule. Hence, using different probes, one obtains a set of such positions which defines a virtual receptor site (VRS). Basically, GRIND are a small set of variables representing the geometrical relationships between relevant regions of the VRS. The procedure for obtaining GRIND involves three steps: (1) computing a set of MIF, (2) filtering the MIF to extract the most relevant nodes, and (3) encoding the filtered MIF into the GRIND variables.

The filtering procedure extracts a set of grid nodes (filtered MIF) on the basis of the energy of the nodes and the distance between them. The filtered nodes are encoded via MACC2 transform into few GRIND variables. Each variable is linked to a grid node-pair placed at a specific distance, and its value refers to the energy values of the linked MIF, which represent attractive interactions between the probe and the molecule.

GRIND variables are organized in correlograms representing either node pairs of the same field (auto-correlo grams) or node pairs of different fields (cross-correlograms). These variables represent the product of the field energy of node pairs that are separated by certain distances in the 3D space of each compound. The alignment-independent GRIND, obtained this way, can be used directly for the chemometric analysis and can be interpreted with the ALMOND software, using graphical representations of the pharmacophoric regions and their mutual distances, together with the molecular structures, in interactive 3D plots.

2.3.3. Statistical approaches. PLS analysis[41] was performed within the software ALMOND. No scaling was applied. The optimal dimensionality of the PLS model was chosen according to the results of crossvalidation. All computations were run on an O2 Silicon Graphics workstation (R 12000).

3. Results and discussion

This section comprises the pharmacological characterization of the 1,4-benzothiazine dataset as well as the derivation of GRIND/ALMOND-based 3D QSAR models. First, binding studies in aortic smooth muscle cells and cardiac membranes of the rat are confronted with formerly measured smooth muscle relaxing data. Then, newly derived 3D QSAR models are compared to previously described qualitative SAR data.

3.1. Smooth muscle relaxing properties

Cecchetti et al.[29] synthesized and biologically evaluated a new series of 1,4-benzothiazine derivatives **3**–**6**, suitably functionalized according to benzopyran-based SAR (Chart 1). K_{ATP}-opening activity was studied in vitro, as the smooth muscle relaxing effect evoked on endothelium-denuded rat aortic rings precontracted with 20 mM KCl.[29] The smooth muscle relaxing potencies, expressed as pEC_{50}, are given in Table 1 as compared to levcromakalim (LCRK); they span an extreme activity spectrum of almost 7 log units ranging from a pEC_{50} of 5.24 for **3aa** to a value of 12.13 for **5c**. The biological data prove that the 1,4-benzothiazine

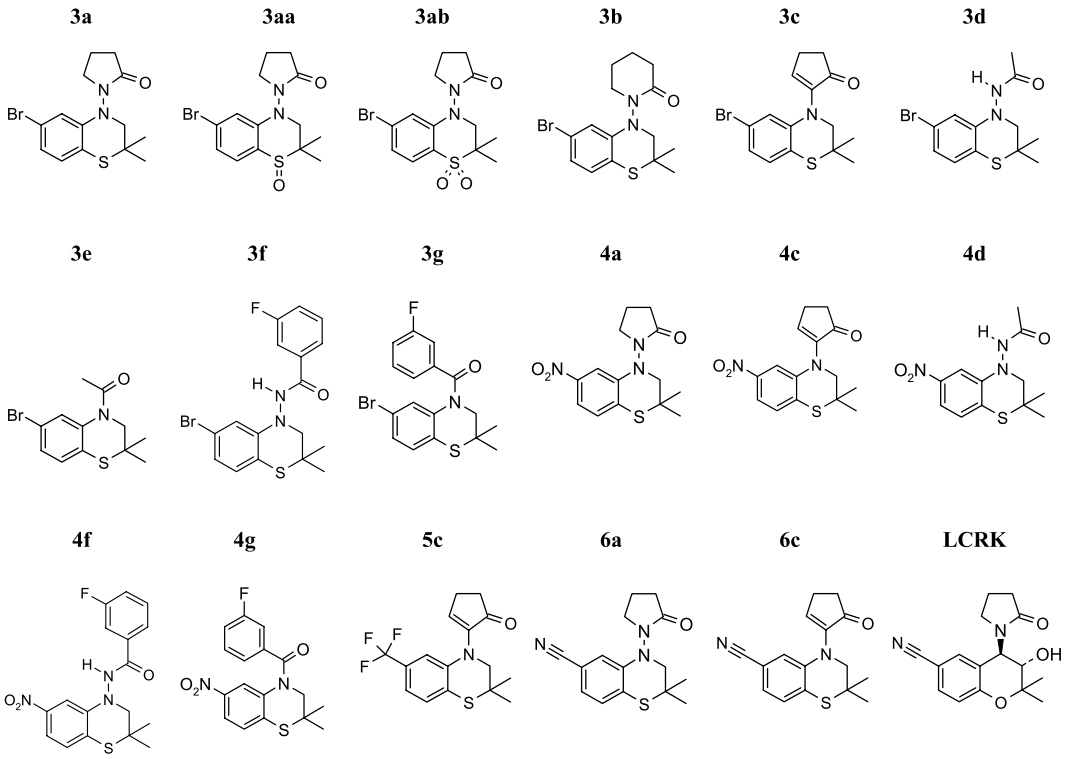

Chart 1. Benzothiazine KCO dataset structures. Cecchetti et al.[29] synthesized this series of 1,4-benzothiazine derivatives **3**–**6**. Compounds are suitably functionalized, according to benzopyran-based SAR, with a *gem*-dimethyl group at C-2 and small C-6 substituents. Furthermore, lactam (**a**, **b**), or cyclopentenone (**c**) rings, acyclic amides (**d**, **f**), and acyl chains (**e**, **g**), all bearing an oxo function at different distances from the benzothiazine nucleus, were selected as N-4 substituents. Additionally, the structure of the reference levcromakalim (LCRK) is given.

nucleus can suitably replace the benzopyran nucleus. The increase in K_{ATP}-opening activity is evident when comparing LCRK with its 1,4-benzothiazine analog **6a**, which was 100 times more potent. 1,4-Benzothiazine derivatives can be considered as structural simplifications of LCRK, due to the absence of chiral centers.

To investigate the mechanism of action, the smooth muscle relaxing potency of some selected compounds was shown to decrease dramatically in high depolarization conditions (aortic rings precontracted with 60 mM KCl), as agrees with a pharmacodynamic profile known for KCOs.[42] Involvement of K_{ATP}-channels in the pharmacological effect was also investigated using the K_{ATP}-blocker glibenclamide. In its presence, the smooth muscle relaxing effects of the test compounds were antagonized competitively, with an almost parallel rightward displacement of the concentration–response curves and an almost full recovery of the maximal effect. These results suggest that the smooth muscle relaxing properties of 1,4-benzothiazines are mediated via K_{ATP}-channels.

3.2. Binding studies to rat aortic vascular smooth muscle cells

To allow comparability with functional data and to quantify the contribution of K_{ATP}-channel binding to smooth muscle relaxation, we performed binding studies in cultured smooth muscle cells of rat aorta using the agonist radioligand [^{3}H]P1075 (for data see Table 1). The reference LCRK, representing the lead benzopyran KCO, exhibits similar constants in both the test systems. Binding affinities of the test compounds span a spectrum of nearly 5 log units ranging from a pK_D-value of 4.76 ± 0.06 for compound **3e** to a pK_D-value of 9.10 ± 0.04 for compound **4c**. Comparison of data for smooth muscle relaxation and binding shows preferentially higher pEC_{50}-values for smooth muscle relaxation; an inverse behavior is found for **3a**, **3ab**, **3b**, and **3d**.

Among the test compounds, 6-nitro substituted pyrrolidones (**a**-series) and cyclopentenones (**c**-series) exhibit the highest, that is, nanomolar affinities; replacement of 6-nitro by cyano reduced affinity by a factor of 6 (0.8 log units). Comparing bromo-substituted compounds at C-6 (**3**) revealed that benzamides and acetamides also are characterized by comparable high affinities with pK_D-values between 7.4 and 7.7 (Table 1). Replacement of Br at C-6 by NO_2 markedly increased affinities by a factor of about 7.5 (acetamides, **d**-series), of about 10 (benzamides **f**-series, pyrrolidones **a**-series), and of about 50 (cyclopentenones, **c**-series). Interestingly, the Br/NO_2-exchange is much more effective in increasing the potency for relaxation as can be seen by comparison of pEC_{50}-values; potencies increased in the **f**-series (benzamides) by a factor of about 30, in the **d**-series (acetamides) by a factor of 100, and in the **c**-series (cyclopentenones) and **a**-series (pyrrolidones) even by a factor of about 1000. These tremendous differences are exclusively caused by an increase

Table 1. Smooth muscle relaxing and radioligand binding data of the benzothiazine KCO dataset

	Aortic rings relaxation pEC_{50}±SEM[a]	Δ (a−b)	RASMC binding pK_D ± ASD[b]	Δ (b−c)	Cardiomyocytes binding pK_D ± ASD[c]
Pyrrolidones					
3a	6.91 ± 0.05	−(0.67 ± 0.08)	7.58 ± 0.07	(1.28 ± 0.08)	6.30 ± 0.03
4a[d]	9.84 ± 0.15[d]	(1.13 ± 0.17)	8.71 ± 0.074	(1.12 ± 0.09)	7.59 ± 0.05
6a	9.27 ± 0.18	(1.59 ± 0.18)	7.68 ± 0.03	(0.91 ± 0.04)	6.77 ± 0.05
3aa	5.24 ± 0.09	(0.02 ± 0.10)	5.22 ± 0.05	(0.66 ± 0.11)	4.56 ± 0.09
3ab	5.49 ± 0.06	−(0.26 ± 0.07)	5.75 ± 0.03	(1.01 ± 0.08)	4.74 ± 0.07
Piperidone					
3b	6.29 ± 0.05	−(0.94 ± 0.06)	7.23 ± 0.04	(1.26 ± 0.08)	5.97 ± 0.07
Cyclopentenones					
3c	7.72 ± 0.16	(0.31 ± 0.17)	7.41 ± 0.04	(0.90 ± 0.09)	6.51 ± 0.08
4c	10.89 ± 0.02	(1.79 ± 0.04)	9.10 ± 0.04	(0.94 ± 0.07)	8.16 ± 0.06
5c	12.13 ± 0.13	(3.84 ± 0.14)	8.29 ± 0.05	(1.05 ± 0.07)	7.24 ± 0.05
6c	11.30 ± 0.13	(3.00 ± 0.14)	8.30 ± 0.05	(1.01 ± 0.09)	7.29 ± 0.08
Acetamides					
3d	7.06 ± 0.11	−(0.39 ± 0.12)	7.45 ± 0.04	(0.92 ± 0.07)	6.53 ± 0.05
4d	9.13 ± 0.07	(0.79 ± 0.09)	8.32 ± 0.05	(1.09 ± 0.08)	7.23 ± 0.06
Acetyl					
3e	5.73 ± 0.04	(0.97 ± 0.07)	4.76 ± 0.06	(0.55 ± 0.08)	4.21 ± 0.05
Benzamides					
3f	7.75 ± 0.07	(0.23 ± 0.09)	7.52 ± 0.06	(1.41 ± 0.08)	6.11 ± 0.06
4f	9.25 ± 0.06	(0.71 ± 0.07)	8.54 ± 0.03	(1.05 ± 0.06)	7.49 ± 0.05
Benzoyls					
3g	5.36 ± 0.40	(0.27 ± 0.43)	5.09 ± 0.17	(0.79 ± 0.19)	4.30 ± 0.10
4g	—	—	5.22 ± 0.07	(0.60 ± 0.12)	4.62 ± 0.09
LCRK	6.98 ± 0.11	−(0.43 ± 0.13)	7.41 ± 0.06	(0.56 ± 0.10)	6.85 ± 0.07

[a] The smooth muscle relaxing potency was evaluated on endothelium-denuded isolated aortic rings of male normotensive Wistar rats. Potency is expressed as mean pEC_{50} ± SEM (−log *M*); all data stem from Cecchetti et al.[29]

[b] Dissociation constants (pK_D, −log *M*) measured as binding competition of [^{3}H]P1075 in cultured aortic smooth muscle cells (RASMC, b); pK_D-values and asymptotic standard deviations (ASD) were estimated by non-linear regression. Differences (Δ) between pEC_{50}-values in aortic rings and pK_D-values in RASMC (Δ a−b) are given in brackets.

[c] Dissociation constants (pK_D, −log *M*) measured as binding competition of [^{3}H]P1075 in disaggregated cardiomyocytes (c) of the rat; pK_D-values and asymptotic standard deviations (ASD) were estimated by non-linear regression. Differences (Δ) between pK_D-values in RASMC and cardiomyocytes (Δ b−c) are given in brackets.

[d] See Ref. 29.

in affinities of the NO_2-derivatives, whereas the Br-derivatives are equipotent in binding and relaxation (cyclopentenones **c**, benzamides **f**) of even less potent in relaxation (pyrrolidones **a**, acetamides **d**). The latter effect can be understood only by assuming that not only affinity (as determined in radioligand binding) but also efficacy as a measure of the conformational change of K_{ATP}-channels combined with a more effective signal transduction contributes to the high efficiency of NO_2-derivatives in smooth muscle relaxation.

A regression analysis correlating binding data (pK_D) and pEC_{50}-values for relaxation (Fig. 1) results in the following equation:

$$pEC_{50} = 1.39(\pm 0.24)pK_D - 2.06(\pm 1.77)$$
$$n = 15, \quad r^2 = 0.841, \quad F = 33.8, \quad s = 1.2551 \qquad (2)$$

Obviously, the high-affinity compounds of the pyrrolidone series (**a**) and the cyclopentenone series (**c**) predominantly contribute to the steepening of the regression, whereas the low-affinity sulfoxide- (**3aa**, **3ab**), acetyl- (**3e**), and benzoyl-(**3g**) derivatives are close to the bisecting line representing matching pEC_{50}- and pK_D-values. That is why the dataset was restricted to the high-affinity compounds excluding the compounds **3aa**, **3ab**, **3e**, and **3g**. The restricted dataset is characterized by the following equation:

$$pEC_{50} = 2.39(\pm 0.66)pK_D - 10.08(\pm 5.27)$$
$$n = 11, \quad r^2 = 0.753, \quad F = 13.1, \quad s = 1.2858 \qquad (3)$$

The steepening of the slope up to 2.39 is essentially caused by the cyclopentenone (**c**)-derivatives. The differences of pK_D- and pEC_{50}-values amount up to three orders of magnitude (Table 1) possibly hinting at a contribution of different signal transduction mechanisms.

3.3. Binding studies to rat cardiomyocytes

Former binding studies with benzopyran KCOs have consistently shown higher affinities to aortic smooth muscle cells than to enzymatically disaggregated heart muscle cells.[43] Also with the reference compound LCRK (Table 1), the affinity for K_{ATP}-channels of RASMC was approximately threefold higher than that for K_{ATP}-channels of cardiomyocytes reflecting the differ-

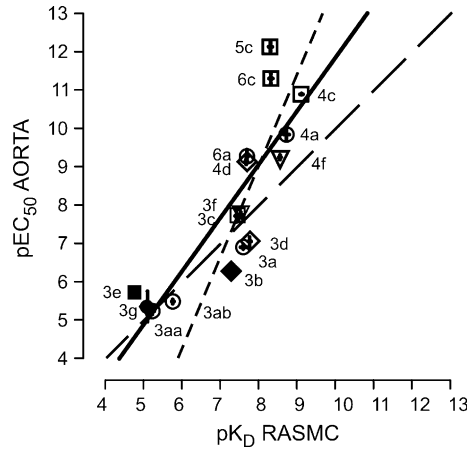

Figure 1. Correlation of the smooth muscle relaxing potencies (pEC_{50} values) of the dataset compounds, measured on endothelium-denuded rat aortic rings precontracted with 20 mM KCl versus their binding affinities (pK_D values), measured in rat aortic smooth muscle cells (RASMC). The dataset is given in Table 1. The thick line represents the regression of the complete dataset. The bisecting line (dashed line) indicates matching pEC_{50}- and pK_D-values, which indeed can be observed with the compounds of series **3** (substituted with Br in C-6). The thin dotted line represents a regression based on the dataset restricted to the high affinity compounds, that is, without the sulfoxide compounds (**3aa** and **3ab**) and without the acetyl- (**3e**) and the benzoyl- (**3g**) derivatives.

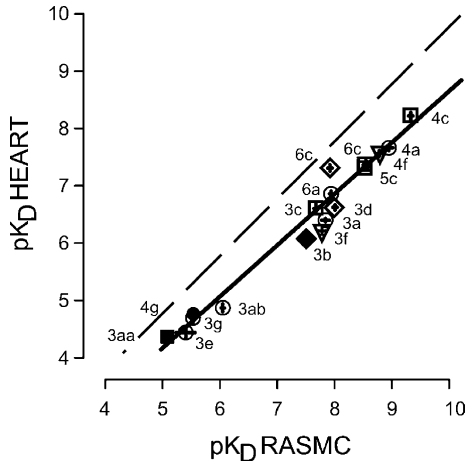

Figure 2. Correlation of the binding affinities of the dataset compounds, measured in cultured smooth muscle cells of rat aorta versus their binding affinities, measured in cardiomyocytes of the rat. The dataset is given in Table 1. The bisecting line (dashed) represents the identity of pK_D-values in heart and smooth muscle cells. Compared to the bisecting line, the regression line (full line) is shifted by 0.5–1.0 log units towards lower affinities in cardiomyocytes.

ences of affinities for SUR2A and SUR2B, which are thought to constitute the cardiac and the smooth muscle type of K_{ATP}-channels.[44] To investigate this relation also for the new chemotype of 1,4-benzothiazine KCOs, we performed binding studies in cardiomyocytes of the rat using [^{3}H]P1075 as a radioligand. In cardiomyocytes, dissociation constants (pK_D) spanned ~4.0 log units ranging from 4.21 ± 0.05 for the weakest compound **3e** to 8.16 ± 0.06 for the most potent compound **4c**.

Similar to binding affinities in smooth muscle cells, also in cardiomyocytes the benzamide-derivatives (**f**-series), the pyrrolidone-derivatives (**a**-series), the cyclopentenone-derivatives (**c**-series), and acetamide-derivatives (**d**-series) were characterized with much higher affinities than the acetyl-derivative **3e** and the benzoyl-derivatives (**g**-series). Within each series, the nitro-derivatives exhibited ~10–40-fold higher affinity than the bromo-derivatives. A similar finding was made comparing the bromo- and the nitro-derivatives of the pyrrolidone-series. Oxidation of the benzothiazine to an oxide (**3aa**) and to a dioxide (**3ab**) induced a dramatic, 40–60-fold loss of affinity (Table 1).

Among the tested compounds, the nitro-derivative **4c** stands out as that one with the highest affinity; the same finding was made with **4c** in aortic smooth muscle cells (Table 1). Within the cyclopentenone-series, the trifluoromethyl (**5c**)- and the cyano (**6c**)-derivatives lose ~5-fold in affinity in comparison with the nitro-derivative **4c**. The correlation of binding data on cardiomyocytes and on cultivated smooth muscle cells resulted in the following relation (see also Fig. 2)

$$pK_D(\text{cardiomyocytes}) = 0.898(\pm 0.043)pK_D(\text{RASMC}) - 0.222(\pm 0.316)$$

$$n = 16,\quad r^2 = 0.983,\quad F = 429.5,\quad s = 0.2430 \qquad (4)$$

This highly significant correlation between these pK_D-values hints at close structural similarities between cardiac K_{ATP}-channels (presumably SUR2A) and aortic smooth muscle K_{ATP}-channels (presumably SUR2B).

3.4. Qualitative SAR

Qualitative SAR of 1,4-benzothiazines[29] can be summarized briefly as follows: C-6 and N-4 substituents play a key role in activity modulation in analogy to benzopyran-based SAR.

Regarding N-4 position, the cyclopentenone containing compounds **4c**, **5c**, and **6c** exhibit the highest activity levels exceeding at least 10,000 times that of LCRK. The strong impact of cyclopentenone is peculiar to the 1,4-benzothiazine series; in the 1,4-benzoxazine series, the same moiety increases the activity but to a lesser extent.[45] The expansion of a five- to a six-membered lactam slightly decreased the activity (**3a** ↔ **3b**). The lactam ring can be replaced by acyclic amido groups to afford compounds with smooth muscle relaxing potencies in the range of LCRK, as in the case of **4d**, **3f**, and **4f**. On the contrary, replacing the acyclic amido by a keto group (**3e**, **3g**, and **4g**) drastically reduces the activity (compare **3d**, **3f**, and **4f**).

In C-6 position, a few electron-withdrawing groups such as both 6-bromo and 6-nitro were inserted. The presence of a 6-Br, coupled with a suitable N-4 substituent, afforded compounds with good smooth muscle relaxing potency in the range of that of LCRK. However, the 6-NO_2 derivatives had a higher activity than their 6-Br

counterparts (**4a** vs **3a**, **4c** vs **3c**, **4d** vs **3d**, and **4f** vs **3f**). Similar to the NO_2 group, CF_3 or CN groups confer very high activity levels as in compounds **5c**, **6a**, and **6c**.

Regarding 1-position, the oxidation of a sulfur atom to sulfoxide as in **3aa** caused a 40-fold decrease in potency, but a further oxidation to sulfone, as in **3ab**, determined a slight recovery of potency. This is in agreement with that already observed by Matsumoto et al.[45]

3.5. Derivation of GRIND/ALMOND-based 3D QSAR models

For 3D QSAR modeling, compounds were described using the alignment-independent GRIND descriptors,[30] derived from GRID MIF. Usually, MIF are directly obtained within the ALMOND software; and for QSAR purposes, the most commonly used GRID probes are DRY (hydrophobic), N1 (hydrogen bond (HB) donor interaction), O (HB acceptor interaction), and TIP (shape description).[46] The X-space of GRIND descriptors was used for multivariate statistics via partial least squares (PLS), since the Y-space of biological activities comprised smooth muscle relaxing potencies and binding affinities, as listed in Table 1.

3.5.1. Chemometric model building. A first run of the GRIND procedure using all four above-mentioned probes revealed that both the block O–O and the cross-blocks O–N1, O–DRY, and O–TIP had only a marginal impact on all the three models. The marginal impact of the probe O is due to the low number of HB donors within the series; only a few molecules exhibit maximally one HB donor. Hence, in the further analysis, only the probes DRY, N1, and TIP were used, in order to gain better results (the probe O produced only noise) and to simplify discussion.

In addition, we noticed that the HB acceptor character of the CF_3 group of compound **5c** was completely neglected by the filtering procedure. Thus, in the coordinate input file for GRIND (KOUT file) of **5c**, we manually modified the HB minimum energy parameter (EMIN value) of fluorines from CF_3 from -0.7 to -1.8 (which represents a low HB character) to ensure the selection of few nodes from that region. Moreover, the number of nodes was set to 50 instead of the default value 100, considering the rather small size of the compounds. When using a lower number of nodes, it is important to 'catch' all the regions around the molecule, when selecting the filtered points. To achieve this, we augmented the relevance of distance on cost of the energy value: the field weight was set to 20% instead of the default value 50%.

For variable selection via fractional factorial design (FFD), we used six random groups (each containing three compounds) and a high value of the combination/variables ratio to find the highest number of fixed variables with a single FFD run. The number of active variables was initially 181 for all the three models. After FFD variable selection, active variables were 123 for smooth muscle relaxation, 102 for RASMC-binding, and 95 for cardiomyocytes-binding. Despite the slightly different number of active variables, which depend mainly on the objects used for modeling and on the relationships found between activity data and GRIND descriptors, the three models could be compared.

Using the above settings, PLS analysis resulted in models of two latent variables for all three biological activities studied; see also Table 2 and Figure 3. Determination coefficients of 0.97 (smooth muscle relaxation) and 0.94 in the case of RASMC-binding and cardiomyocytes-binding affinities were found. Internal validation of these models was performed using the same validation method: q^2 values of the validated models were 0.69, 0.66, and 0.64, respectively. All three models were statistically good, both in fitting and in internal validation. Owing to the low number of compounds, external validation could not be carried out.

Binding data are clearly split into two subgroups of 5 and 13 compounds, respectively. Compounds **3e**, **3g**, **3aa**, **4g**, and **3ab** are characterized by weak binding to cardiomyocytes and to smooth muscle cells; they are grouped on the left side of the corresponding plots in Figures 3b and c. Conversely, a unique overall trend was observed for relaxation data, for which the distribution of values was almost uniform (Fig. 3a) although two subgroups of 10 and 7 compounds could be identified. In fact, low relaxation values are assumed by levcromakalim and all **3**-compounds, whereas **4**-, **5**-, and **6**-compounds assume higher relaxation values. The same subgroups were evident when we reported the regression analysis of aortic relaxation versus smooth muscle cells binding (Fig. 1).

Table 2. Statistics of PLS models for smooth muscle relaxation, RASMC binding and cardiomyocytes binding

LV	Smooth muscle relaxation				RASMC binding				Cardiomyocytes binding			
	r^2	q^2	SDEC	SDEP	r^2	q^2	SDEC	SDEP	r^2	q^2	SDEC	SDEP
1	0.90	0.51	0.66	1.48	0.82	0.51	0.56	0.94	0.85	0.44	0.47	0.91
2	**0.97**	**0.69**	**0.37**	**1.18**	**0.94**	**0.66**	**0.34**	**0.78**	**0.94**	**0.64**	**0.29**	**0.73**
3	0.99	0.74	0.26	1.08	0.99	0.74	0.16	0.69	0.98	0.72	0.16	0.65

All the statistics [r^2 and q^2 values as well as standard deviation of error calculation (SDEC) and Prediction (SDEP)] reported here refer to PLS models obtained after the first run of FFD variable selection using the following settings: Max.dim.: 3; 6 random groups; 20 SDEP; recalculated weights; retain uncertain variables; 20% dummies; Comb/Var ratio = 5. The same validation method is used to calculate q^2 and SDEP. Values of q^2, increasing with higher numbers of LV, might suggest the use of more complex model, but we considered two-LV models (bold) satisfactory due to the marginal improvement in statistical data when using 3LV.

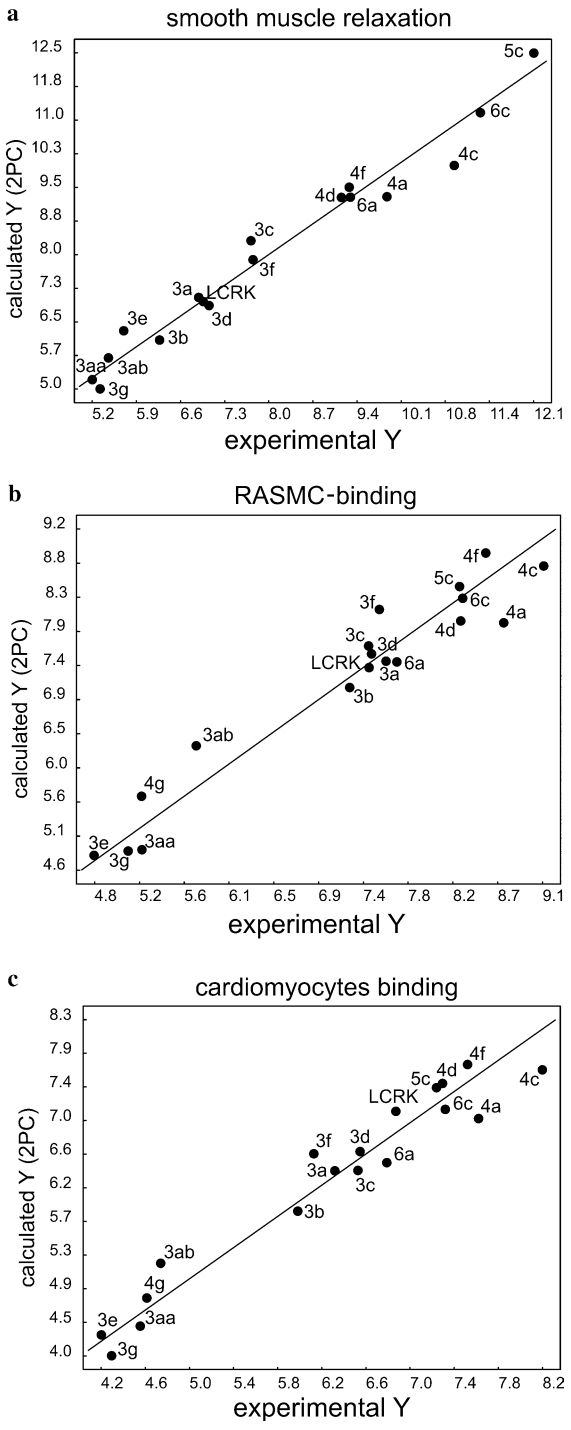

Figure 3. Calculated versus experimental values for the three models: smooth muscle relaxation (a), RASMC-binding (b), and cardiomyocytes binding (c).

To gain a deeper insight into the models, the variables with highest impact on the biological activities were inspected in more detail. Their coefficients are comparatively plotted in a color-coded way for smooth muscle relaxation (black) and RASMC-binding (grey) in Figure 4, where capital letters indicate the peaks of largest importance. The interpretation of the relevant peaks is summarized in Table 3 for all three activities. Node-pairs and peak codes of the most relevant variables, and their impact on the three PLS models are listed to highlight similarities and differences between the models. The analysis of the mentioned variables allowed to encode the filtered MIF into regions, which were recognized as relevant for at least one model. From the MIF obtained with the probes N1, DRY, and TIP the regions listed in Table 4 were identified. The carbonyl on the substituent at N-4, the HB acceptor at C-6, the five-membered ring at N-4, and the *gem*-dimethyl group resulted as the main structural features responsible for strong binding as well as for strong smooth muscle relaxation. All these features are shown as example for compound **5c** in Figure 5, where it is reported together with its MIF and some distances which were found to be relevant for the models.

On the other hand, it was rather difficult to detect variables, and thereby structural features responsible for differences between the models. Therefore, the attention was focused on the probes, and a sort of consensus of each probe was obtained by excluding all the three probes one-by-one. This way we obtained several PLS models with reduced numbers of probes (two) and consequently reduced numbers of variables. For example, when excluding the probe DRY from all three models, only the probes N1 and TIP were used for modeling; the resulting PLS models were internally validated and consistent models were still obtained. Therefore, the exclusion of the DRY probe is not detrimental for any of the models. Conversely, when excluding N1 or TIP probes from the three models, different results arose for binding and relaxation data. The smooth muscle relaxation model was still consistent, and both of these probes could be eliminated without highly compromising the model. Conversely, the same probes are highly relevant for both the binding models, since the q^2 assumed negative values when deleting N1 or TIP. From this analysis, we observed that the relaxation model equivalently depends on the three probes and no extreme detrimental effect emerges when deleting one of them. On the other hand, binding models highly depend on N1 and TIP probes, whereas the DRY probe only slightly affects these models.

4. Conclusion

Binding studies in rat aortic smooth muscle cells and cardiomyocytes, performed in this paper for seventeen 1,4-benzothiazine-type KCOs, revealed broad affinity ranges in both the test systems. Binding affinities in aortic smooth muscle cells span a spectrum of nearly 5 log units ranging from a pK_D-value of 4.76 ± 0.06 for compound **3e** to a pK_D-value of 9.10 ± 0.04 for compound **4c**. In cardiomyocytes, pK_D values spanned ~4 log units ranging from 4.21 ± 0.05 for the weakest compound **3e** to 8.16 ± 0.06 for the most potent compound **4c**. Comparing the binding affinities in rat aortic preparations with previously published smooth muscle relaxation data shows preferentially higher pEC_{50}-values for smooth muscle relaxation. In the most pronounced case of the 6-CF_3 substituted compound **5c**, the pEC_{50} for relaxation surmounts the pK_D value for binding affinity by ~4 log units. This is only understandable when not

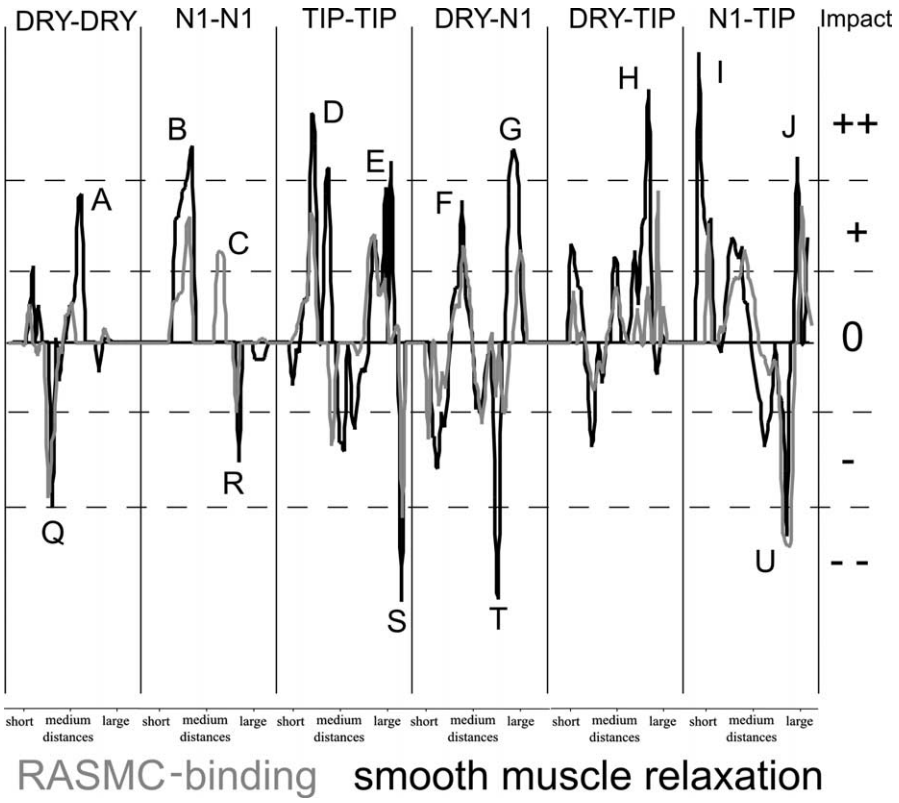

Figure 4. PLS coefficients profiles (2LV) for models of smooth muscle relaxation (black), and RASMC-binding (gray). The impact on the models is schematised by the code + +/+/0 /−/−−, where + + and −− stand for variables which have highly positive or negative impact, whereas + and − stand for lower impact and 0 stands for null or almost null impact on the activity.

Table 3. Model similarities and differences between smooth muscle relaxation (Vas), RASMC and to cardiomyocytes

Probe Block	Similarities					Differences				
	Peak code	Relevant variables[a]	Impact			Peak code	Relevant variables[a]	Impact		
			Vas	RASMC	Cardiomyocytes			Vas	RASMC	Cardiomyocytes
DRY–DRY	Q	13–15	−−	−	−	A	21–22	+	/	/
N1–N1	B[b]	10–15	+ +	+	+	C	23–25	/	+	/
						R	29	−	−	/
TIP–TIP	S	38	−−	−−	−−	D[c]	11–16	+ +	+	+
						E[d]	28–35	+ +	+	+
DRY–N1	F	16–17	+	+	+	U[e]	26–29	−−	−	−
						G[f]	30–34	+ +	+	+
DRY–TIP						H[g]	32,34	+ +	+	+
N1–TIP	J	37	+ +	+ +	+ +	I[h]	7–11	+ +	+	+
	U	31–34	−	−−	−−					

[a] For an estimate of distance in Å, the variable number has to be multiplied by 0.4, which is the product of the grid spacing (0.5 Å) and the smoothing window value (0.8).
[b] For binding peaks have large impact only on variables 14 and 15, whereas for relaxation on the entire interval 10–15.
[c] For binding peaks are referred only to variables 11–12, whereas for relaxation until variable 16.
[d] For binding peaks are referred only to variables 28–30, whereas for relaxation until variables 33–35.
[e] For binding peaks are referred to variables 26–29, whereas for relaxation only to variables 26–27.
[f] For binding peaks have large impact only on variables 32–34, whereas for relaxation on the entire interval 30–34.
[g] For relaxation peak are referred to variable 32, whereas for binding to variable 34.
[h] For relaxation peaks are referred to variables 7–11, whereas for binding only to variables 9–10.

only affinity (as determined in radioligand binding) but also efficacy (as measure for the conformational change of K_{ATP}-channels) combined with a more effective signal transduction contributes to the high efficiency of NO_2-derivatives in smooth muscle relaxation.

In the second part of the study, we derived 3D QSAR models using GRIND/ALMOND descriptors. 3D QSAR analysis resulted in PLS models of two latent variables for all three biological activities. Determination coefficients of 0.97 (smooth muscle relaxation)

Table 4. Regions encoded from MIF and their involvement in peaks relevant on the models

Probe	Region	Peaks
N1	Carbonyl on the substituent at N-4	C, B, F, and I
N1	HB acceptor at C-6 (CN, NO_2, CF_3)	C, B, G, and J
N1	Oxygens of SO (**3aa**) and SO_2 (**3ab**) groups	R and U
N1	Oxygens of acetamides and benzamides	T
DRY	Hydrophobic region over the main ring, reinforced by the axial methyl	A and F
DRY	Hydrophobic region due to the five-membered ring or other substituent at N-4	A, G, and H
TIP	Tip edges due to the five-membered ring at N-4. They suggest a hypothetical loop of the virtual receptor where the five-membered ring fits perfectly. These tip edges are able to differentiate compounds with and without a substituent at position 4 which is not a five-membered ring when involved in peaks D and E	E, D, and I
TIP	Any substituent at C-6	E and H
TIP	Equatorial methyl	E and J

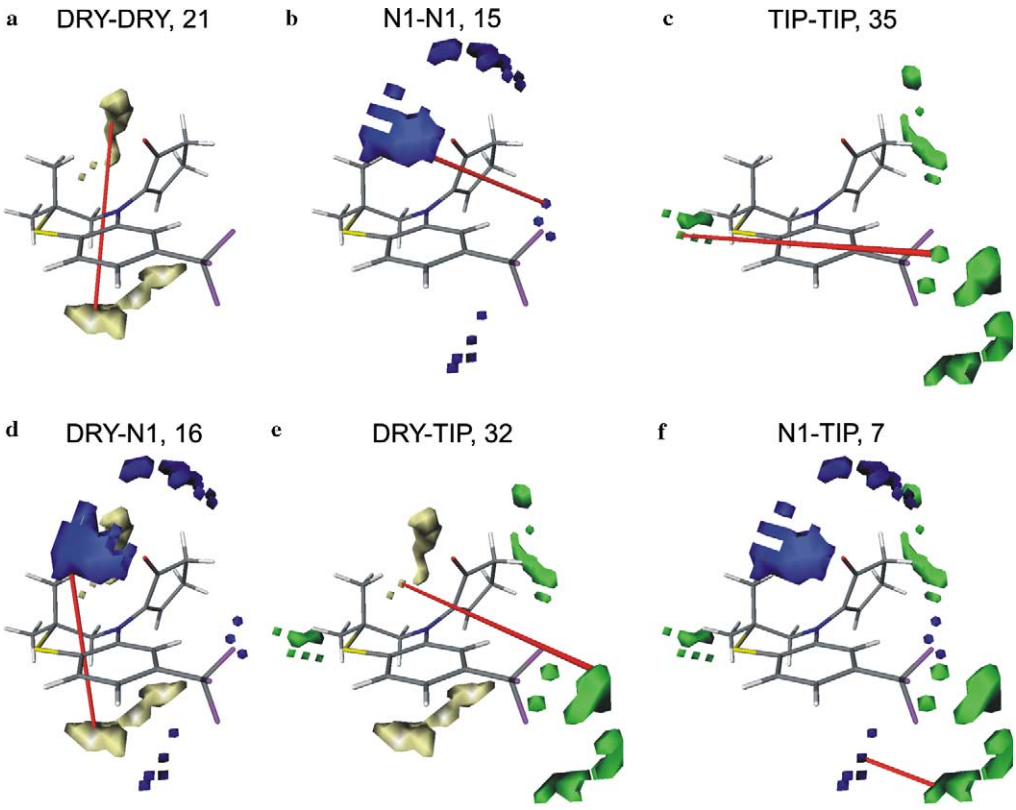

Figure 5. Compound **5c** is used as a reference and is reported with its MIF colored as follows: yellow MIF are for DRY probe; blue MIF are for N1 probe, whereas green MIF are for the TIP probe. Some variables are reported to highlight the MIF related to most of the peaks with positive impact on the models: (a) peak A; (b) peak B; (c) peak E; (d) peak F; (e) peak H; (f) peak I.

and 0.94 (RASMC- and cardiomyocytes-binding) were found. Internal validation of these models yielded q^2 values of 0.69, 0.66, and 0.64, respectively. Main pharmacophoric features for all three activities are the carbonyl on the substituent at N-4, the HB acceptor at C-6, the five-membered ring at N-4, and the geminal dimethyl groups.

Thus, the present data favor the assumption that the above postulated additional mechanism, responsible for the outstanding smooth muscle relaxation potencies, necessitates pharmacophoric features which closely resemble that of K_{ATP}-channel binding.

Acknowledgment

We thank Loriano Storchi, Chemistry Department, University of Perugia, for his help in ab initio calculations.

References and notes

1. Isomoto, S.; Kondo, C.; Kurachi, Y. *Jpn. J. Physiol.* **1997**, *47*, 11.
2. Aguilar-Bryan, L.; Clement, J. P.; Gonzalez, G.; Kunjilwar, K.; Babenko, A.; Bryan, J. *Physiol. Rev.* **1998**, *78*, 227.

3. Faivre, J. F.; Findlay, I. *Biochim. Biophys. Acta* **1990**, *1029*, 167.
4. Noma, A. *Nature* **1983**, *305*, 147.
5. Dunne, W. J.; Petersen, O. H. *Biochim. Biophys. Acta* **1991**, *1071*, 67.
6. Cook, D. L.; Hales, C. N. *Nature* **1984**, *311*, 271.
7. Quayle, J. M.; Standen, N. B. *Cardiovasc. Res.* **1994**, *28*, 797.
8. Standen, N. B.; Quayle, J. M.; Davies, N. W.; Brayden, J. E.; Huang, Y.; Nelson, M. T. *Science* **1989**, *245*, 177.
9. Amoroso, S.; Schmid-Antomarchi, H.; Fosset, M.; Lazdunski, M. *Science* **1990**, *247*, 852.
10. Bernardi, H.; Fosset, M.; Lazdunski, M. *Proc. Natl. Acad. Sci. U.S.A.* **1988**, *85*, 9816.
11. Atwal, K. S. *Med. Res. Rev.* **1992**, *6*, 569.
12. Hamilton, T. C.; Weir, S. W.; Weston, A. H. *Br. J. Pharmacol.* **1986**, *88*, 103.
13. (a) Southerton, J. S.; Taylor, S. G.; Weir, S. W.; Weston, A. H. *Br. J. Pharmacol.* **1987**, *90*, 126P; (b) Bray, K. M.; Newgreen, D. T.; Small, R. C.; Southerton, J. S.; Taylor, S. G.; Weir, S. W.; Weston, A. H. *Br. J. Pharmacol.* **1987**, *91*, 421.
14. Yanagisawa, T.; Taira, N. *Naunyn-Schmiedeberg's Arch. Pharmacol.* **1980**, *312*, 69.
15. Pelaia, G.; Gallelli, L.; Vatrella, A.; Grembiale, R. D.; Maselli, R.; De Sarro, G. B.; Marsico, S. A. *Life Sci.* **2002**, *70*, 977.
16. Wein, A. *J. Exp. Opin. Invest. Drugs* **2001**, *10*, 65.
17. (a) Buhl, A. E.; Waldon, D. J.; Conrad, S. J.; Mulholland, M. J.; Shull, K. L.; Kubicek, M. F.; Johnson, G. A.; Brunden, M. N.; Stefanski, K. J.; Stehle, R. G.; Gadwood, R. C.; Kamdar, B. V.; Thomasco, L. M.; Schostarez, H. J.; Schwartz, T. M.; Diani, A. R. *J. Invest. Dermatol.* **1992**, *98*, 315; (b) Li, M.; Marubayashi, A.; Nakaya, J.; Fukui, K.; Arase, S. *J. Invest. Dermatol.* **2001**, *117*, 1594; (c) Davies, G. C.; Thornton, M. J.; Jenner, T. J.; Chen, Y. J.; Hansen, J. B.; Carr, R. D.; Randall, V. A. *J. Invest. Dermatol.* **2005**, *124*, 686.
18. Grover, G. J.; Garlid, K. D. *J. Mol. Cell. Cardiol.* **2000**, *32*, 677.
19. Szewczyk, A.; Pikula, S. *Biochem. Pharmacol.* **2000**, *60*, 607.
20. Inagaki, N.; Tsuura, Y.; Namba, N.; Masuda, K.; Gonoi, T.; Horie, M.; Seino, Y.; Mizuta, M.; Seino, S. *J. Biol. Chem.* **1995**, *270*, 5691.
21. Sakura, H.; Ämmälä, C.; Smith, P. A.; Gribble, F. M.; Ashcroft, F. M. *FEBS Lett.* **1995**, *377*, 338.
22. Aguilar-Bryan, L.; Nichols, C. G.; Wechsler, S. W.; Clement, J. P., IV; Boyd, A. E.; González, G.; Herrera-Sosa, H.; Nguy, K.; Bryan, J.; Nelson, D. A. *Science* **1995**, *268*, 423.
23. Inagaki, N.; Gonoi, T.; Clement, J. P., IV; Nambe, N.; Inazawa, J.; González, G.; Aguilar-Bryan, L.; Seino, S.; Bryan, J. *Neuron* **1996**, *16*, 1011.
24. Isomoto, S.; Kondo, C.; Yamada, M.; Matsumoto, S.; Higashiguchi, O.; Horio, Y.; Matsuzawa, Y.; Kurachi, Y. *J. Biol. Chem.* **1996**, *271*, 24321.
25. Uhde, I.; Toman, A.; Gross, I.; Schwanstecher, C.; Schwanstecher, M. *J. Biol. Chem.* **1999**, *274*, 28079.
26. Empfield, J. R.; Russell, K. *Annu. Rep. Med. Chem.* **1995**, *30*, 81.
27. Coghlan, M. J.; Carroll, W. A.; Gopalakrishnan, M. *J. Med. Chem.* **2001**, *44*, 1627.
28. Evans, J. M.; Stemp, G. Structure–Activity Relationships of Benzopyran based Potassium Channel Activators. In *Potassium Channels and Their Modulators. From Synthesis to Clinical Experience*; Evans, J. M., Hamilton, T. C., Longman, S. D., Stemp, G., Eds.; Taylor & Francis Ltd: London, 1996, pp 27–55.
29. Cecchetti, V.; Calderone, V.; Tabarrini, O.; Sabatini, S.; Filipponi, E.; Testai, L.; Spogli, R.; Martinotti, E.; Fravolini, A. *J. Med. Chem.* **2003**, *46*, 3670, and relative ''additions and corrections'' submitted..
30. Pastor, M.; Cruciani, G.; McLay, I.; Pickett, S.; Clementi, S. *J. Med. Chem.* **2000**, *43*, 3233.
31. Ross, R. *J. Cell. Biol.* **1971**, *50*, 172.
32. Buxton, I. L.; Brunton, L. L. *J. Biol. Chem.* **1983**, *258*, 10233.
33. Manley, P. W.; Quast, U.; Andres, H.; Bray, K. *J. Med. Chem.* **1993**, *36*, 2004.
34. Quast, U.; Bray, K.; Andres, H.; Manley, P. W.; Baumlin, Y.; Dosogne, J. *Mol. Pharmacol.* **1993**, *43*, 474.
35. Lemoine, H.; Ehle, B.; Kaumann, A. J. *Naunyn-Schmiedeberg's Arch. Pharmacol.* **1985**, *331*, 40.
36. Lemoine, H. *Quant. Struct. Act. Relat.* **1992**, *11*, 211.
37. Frisch, M. J.; Trucks, G. W.; Schlegel, H. B.; Scuseria, G. E.; Robb, M.A.; Cheeseman, J. R.; Zakrzewski, V. G.; Montgomery, Jr., J. A.; Stratmann, R. E.; Burant, J. C.; Dapprich, S.; Millam, J. M.; Daniels, A. D.; Kudin, K. N.; Strain, M. C.; Farkas, O.; Tomasi, J.; Barone, V.; Cossi, M.; Cammi, R.; Mennucci, B.; Pomelli, C.; Adamo, C.; Clifford, S.; Ochterski, J.; Petersson, G. A.; Ayala, P. Y.; Cui, Q.; Morokuma, K.; Malick, D. K.; Rabuck, A. D.; Raghavachari, K.; Foresman, J. B.; Cioslowski, J.; Ortiz, J. V.; Baboul, A. G.; Stefanov, B. B.; Liu, G.; Liashenko, A.; Piskorz, P.; Komaromi, I.; Gomperts, R.; Martin, R. L.; Fox, D. J.; Keith, T.; Al-Laham, M. A.; Peng, C. Y.; Nanayakkara, A.; Gonzalez, C.; Challacombe, M.; Gill, P. M. W.; Johnson, B.; Chen, W.; Wong, M. W.; Andres, J. L.; Gonzalez, C.; Head-Gordon, M.; Replogle, E. S.; Pople, J. A. Gaussian 98, Revision A.7, Gaussian: Pittsburgh PA, 1998.
38. Becke, A. D. *J. Chem. Phys.* **1993**, *98*, 5648.
39. Version 3.3 of the software ALMOND is available from Molecular Discovery Ltd., 215 Marsh Road, HA5 5NE, Pinner, Middlesex, UK. http://www.moldiscovery.com.
40. (a) Goodford, P. *J. Med. Chem.* **1985**, *28*, 849; (b) Carosati, E.; Sciabola, S.; Cruciani, G. *J. Med. Chem.* **2004**, *47*, 5114.
41. Wold, S.; Albano, C.; Dunn, III, W. J.; Edlund, U.; Esbensen, K.; Geladi, P.; Hellberg, S.; Johansson, E.; Lindberg, W.; Sjostrom, M. In *Chemometrics: Mathematical and Statistics in Chemistry*, Kowalsky, B. R., Ed.; D. Reidel Publishing Company: Dordrecht, Holland, 1983.
42. Magnon, M.; Calderone, V.; Floch, A.; Cavero, I. *Naunyn-Schmiedeberg's Arch. Pharmacol.* **1998**, *358*, 452.
43. Salamon, E.; Mannhold, R.; Weber, H.; Lemoine, H.; Frank, W. *J. Med. Chem.* **2002**, *45*, 1086.
44. Schwanstecher, M.; Sieverding, C.; Dörschner, H.; Gross, I.; Aguilar-Bryan, L.; Schwanstecher, C.; Bryan, J. *EMBO J.* **1998**, *17*, 5529.
45. Matsumoto, Y.; Tsuzuki, R.; Matsuhisa, A.; Takayama, K.; Yoden, T.; Uchida, W.; Asano, M.; Fujita, S.; Yanagisawa, I.; Fujikura, T. *Chem. Pharm. Bull.* **1996**, *44*, 103.
46. Fontaine, F.; Pastor, M.; Sanz, F. *J. Med. Chem.* **2004**, *47*, 2805.